Research on Driving Waveform and Residual Oscillation in Piezo Inkjet

WU Qiu-min
Xi'an University of Technology
CUI Xin-yu (cxy18047122573@163.com)
Xi'an University of Technology https://orcid.org/0000-0002-2834-7642
XU Lei
Xi'an University of Technology
SU Xin
Xi'an University of Technology

Research

Keywords: Piezoelectric inkjet printing, Residual oscillations, Driving waveform

Posted Date: February 2nd, 2022

DOI: https://doi.org/10.21203/rs.3.rs-1221582/v1

Abstract

Piezoelectric driving system is an important part in inkjet printing equipment. The driving waveform, the structure of print head, and etc., directly affect the ejection characteristics and the printing accuracy of droplets. In this paper, the driving waveform was taken as the research object, then established a finite element analysis model for driving droplet ejection, the influence of each time component (voltage rise time t_{rise}, voltage falling time t_{fall} and voltage dwell time t_{dwell}) of trapezoidal wave on the displacement of the driver and the pressure at the nozzle orifice was studied and optimized. According to the two-phase flow model of the nozzle developed, the relationship between driving parameters (voltage amplitude, voltage dwell time t_{dwell}, and operating frequency) and jetting characteristics (droplet velocity and volume) was obtained. Finally, a bipolar driving waveform was designed to suppress the residual oscillation. The results show that the damping waveform can effectively suppress the residual vibration of the pressure wave and greatly improve the working frequency and printing accuracy of the inkjet printing head.

1 Introduction

In inkjet printing, computer is used to convert images and character information into electrical signals, then under the control of electrical signal, the droplets are ejected to the substrate and complete the printing process [1]. Piezoelectric inkjet has become the most promising printing technology in modern times because of its high precision, high efficiency, environmental protection and wide material compatibility. It has been widely used in many industrial fields such as large-scale inkjet printing, printing electronics, biomedicine, additive manufacturing and so on [2–7].

In the process of piezoelectric inkjet printing, the piezoelectric driver deforms under the action of the driving voltage and generates a pressure wave in the chamber.When the pressure wave at the nozzle orifice is large enough, the ink will overcome the resistance and eject from the nozzle orifice and finally form the ink droplets.When the ink is ejected by a pressure wave,the residual pressure wave in the ink channel takes a while to decay,if the next ink droplet is driven before the pressure wave is completely attenuated, the flight speed and volume of the droplet will be affected obviously, and even secondary ejection will be produced [8].Therefore, to study the characteristics of residual oscillation of pressure wave and accelerate its attenuation process,it is of great significance to improve the ejection speed and the consistency of ink droplets.In recent years,many scholars have studied the influence of driving waveform and driving parameters on droplet jet characteristics.Gan H Y et al. used a circular piezoelectric element to drive the nozzle inkjet system, and studied the influence of various waveforms on the volume of ink drops, including monopole wave, bipolar wave, M-wave and W-wave [9].Shin et al. used experiments to study the influence of time interval and driving voltage in double waveform on the volume and velocity of low viscosity fluid ink drop, and obtained the ideal ink drop by changing the time interval and voltage [10].Amol A. Khalate et al. optimized the driving waveform of the piezoelectric print head based on the robust feedforward control method and proved that the waveform designed by this method could

effectively suppress the residual oscillation of the pressure wave through simulation analysis and experimental research [11].

The piezoelectric inkjet process involves the coupling of multiple physical fields such as piezoelectric domain, solid domain, fluid domain, and gas-liquid two-phase flow. In the numerical analysis in this paper, the piezoelectric driver model, piezoelectric print head model and nozzle two-phase flow model of the piezoelectric inkjet system were established respectively. Innovatively, the fluid velocity at the nozzle inlet calculated by the piezoelectric inkjet print head model is introduced into the nozzle two-phase flow model as the inlet condition, and then couple the two models together to form a complete piezoelectric inkjet printing system model. The process of droplets forming and its influencing factors were studied systematically, as shown in Figure 1 and Figure 2[12]. In addition, the influence of residual oscillation on droplet jetting characteristics of the piezoelectric inkjet system is studied, and a new driving waveform is designed to suppress the residual oscillation. It is showed that the working frequency of the piezoelectric inkjet system is improved, and the efficient and stable ejection of droplets is realized.

2 Optimization Of The Driving Waveform

Productivity and stability are important requirements in printing, which are closely related to the jetting process. Driving waveform is one of the most important parameters which play a central role in the printing process. In this paper, the classic trapezoidal driving waveform was studied and optimized. As shown in Figure 3, the trapezoidal wave is composed of three parameters: voltage rise time t_{rise}, voltage dwell time t_{dwell}, and voltage fall time t_{fall}. Among them, voltage dwell time t_{dwell} is a key parameter that affects ink droplet jetting characteristics deeply.

2.1 Analysis and Optimization of Voltage Rise Time t_{rise}

During the voltage rise stage, the piezoelectric actuator bends upwards, causing the pressure chamber to increase in volume and generate negative pressure, which will move to both sides of the chamber.The voltage rise time (t_{rise}) is related to the displacement of piezoelectric actuator, the velocity and pressure of the fluid at the nozzle. The piezoelectric driver model (in Figure 1) is used for numerical calculation, and the simulation results are shownin Figure 4.As t_{rise} increases, the displacement of the driver and the time to reach the peak increase correspondingly. However, the overall trend does not change much, which means that although t_{rise} is different, their ink absorption capacity is similar.Figure 5 shows the pressure-time curve at the nozzle corresponding to different t_{rise} values.With different t_{rise}, the pressure changed significantly only at the peak of the first negative pressure.As t_{rise} increases, the rate of voltage rise decreases, and the deformation of the driver slows down, resulting in lower velocity and pressure of the fluid at the nozzle orifice.Thus, t_{rise} is finally determined to be 4μs.

2.2 Analysis and Optimization of Voltage Fall Time t_{fall}

According to the wave conduction theory, during the voltage fall stage, piezoelectric actuator returns its initial position, and the volume of the pressure chamber is reduced to generate a positive pressure, which is superimposed with the pressure wave reflected in the voltage rise stage. As a result, the positive pressure wave increases and the negative pressure wave disappears. When the strengthened positive pressure wave arrives at the nozzle, the flow at the nozzle will be jetted at a high speed. This stage is called ink-jet stage. Therefore, the goal of t_{fall} optimization is to promote the fluid velocity and pressure at the nozzle orifice as much as possible.

It can be seen from Figure 6 that as the voltage fall time t_{fall} increases, the fluid velocity at the nozzle increases first and then decreases, and it reaches the maximum value at 3μs. When t_{fall} increases, the pressure at the nozzle orifice is different at the first positive pressure wave, and as t_{fall} gradually increases, the first positive pressure gradually decreases. In order to obtain a higher droplet jetting speed, t_{fall} is finally determined as 3μs, as shown in Figure 7.

2.3 Analysis and Optimization of Voltage Dwell Time t_{dwell}

During the voltage dwell stage, the negative pressure wave generated in the voltage rising stage will propagate and reflect in the chamber. Afterwards, the positive pressure wave generated during the voltage fall stage is superimposed or canceled, the length of the t_{dwell} determines the mutual superposition or cancellation effect between the pressure waves. When the enhanced positive pressure wave reaches the nozzle, the fluid in the nozzle will be jetted at a high speed, and the high-speed jetting of the ink droplets will be realized with a smaller driving force. The specific time to form the positive peak value of the velocity wave was calculated by using the piezoelectric inkjet printhead model and obtained t_{dwell} = 8μs.

The effects of t_{dwell} on the fluid velocity at the nozzle is shown in Figure 8. With the increase of t_{dwell}, the fluid velocity increases at first and then decreases, and reaches the maximum when t_{dwell} is 8μs. If t_{dwell} is too large or too small, the pressure waves generated during the voltage rise and fall stage will be canceled each other out, and then the pressure at the nozzle orifice is reduced, thereby causing the fluid velocity slows down. The results are consistent with those obtained by using the velocity wave superposition principle.

3 Effects Of Driving Parameters On Jetting Characteristics Of The Ink Droplet

The driving parameters such as voltage amplitude, voltage dwell time t_{dwell}, and operating frequency have greatest influence on the jetting characteristics of the ink droplet. Therefore, the relationship between driving parameters and jetting characteristics will be studied from three parameters above.

3.1 Driving voltage amplitude

The driving voltage amplitude determines the energy to fire a droplet and influences the ink jetting speed and flow rate. According to the two-phase flow model of nozzle developed in Figure 2, the simulation

results are shown in Figure 9 and 10. It can be seen that with the increase of driving voltage amplitude, the length of the liquid column increases, and the flight speed and volume of the ink droplets increase, too. When the driving voltage increases, the displacement of the piezoelectric actuator increases. This results in greater pressure waves inside the channel. In a given printhead, the greater the pressure, the greater the flow velocity and flow rate at the nozzle orifice.

For example, when the driving voltage is 40V, the liquid column is longer, and the ink droplets have a longer tail after breaking. The satellite ink droplets will be formed after the tail is broken. And the longer the tail, the larger the number and volume of satellite droplets. When the driving voltage is 10V, there is no ink drop ejection. This is because the driving voltage is too small, and the fluid in the channel cannot obtain enough energy to overcome the resistance caused by factors such as viscosity and surface tension, and thus cannot be ejected from the nozzle to form a droplet. Therefore, a smaller driving voltage is chosen to improve the droplet forming quality and ejection stability.

3.2 Voltage dwell time

It can be seen from the simulation results in Figure 11 and 12, with the voltage dwell time t_{dwell} increases, the droplet velocity and volume increase at first and then decrease. When t_{dwell}=8μs, the length of liquid column is the longest, and the speed and volume of the droplet reach the maximum. It shows that when t_{dwell}=8μs, the positive pressure peak generated, which makes the fluid in channel obtain higher pressure under the same driving conditions.

3.3 Operating frequency

The productivity is directly related to the maximum frequency at which the printhead can be operated, so the operating frequency also determines the performance of the printhead. The simulation results of jetting effect on operating frequency are shown in Figure 13. When the frequency varies from 5 KHz to 10 KHz, the droplets ejected effectively, and no satellite droplet appears. After that, when the frequency increases gradually, the droplet ejection speed increases, and the number of satellite droplets increases gradually, too, which will affect the print quality.

4 Waveform Design To Suppress The Residual Oscillations

After a droplet has been ejected from the nozzle, the pressure waves responsible still run through the channel of printhead. These oscillations are called residual oscillations. The time required to damp the residual oscillations depends on the geometry and material properties of the channel and the viscosity of the ink.

Figure 14 shows the comparison between the ideal fluid velocity and the actual fluid velocity in channel. After the ink droplet is ejected (red dot), the residual pressure wave propagating in the channel, the time required to damp the residual oscillations is about 130 μs. The ideal fluid velocity without residual oscillation is shown by the blue dotted line in the figure, the residual pressure wave in the printhead dissipates quickly after the ink droplets ejected and had no effects on the ejection of next droplets. In

fact, when a jetting pulse is applied before the residual oscillations (generated by the previous drop) are damped completely, the drop properties of the jetted drop will be different from the previous drop. Consequently, the total pressure in the channel and, the droplet speed and volume depend also on the time between the two jetting pulses. Therefore, it is of great significance to study the characteristics of the residual oscillation and accelerate the attenuation process of the residual oscillation to improve the jetting velocity and the consistency of the droplets.

4.1 Damping waveform design

In order to accelerate the attenuation of residual oscillations, a bipolar driving waveform is designed, which is shown in Figure 15. Based on the standard waveform, an auxiliary damping waveform is added to accelerate the attenuation of residual oscillations. The parameters include: t_{rR}, t_{fR}, t_{rQ}, t_{fQ} are the rise and fall times of the waveform respectively, t_{dR} is the voltage dwell time of the first standard waveform, t_d is the time interval between the damping waveform and the standard waveform, t_{dQ} is the voltage dwell time of the damping waveform, and U_R and U_Q are the voltage amplitudes of the standard waveform and the damping waveform, respectively, as shown in Figure 15.

As shown in Figure16, according to the principle of wave superposition, when the velocity at the nozzle is restored from the first positive peak to zero, the damping waveform is loaded on the piezoelectric actuator, and then the pressure wave generated by damping waveform will neutralize the residual pressure wave. The standard waveform is mainly used to generate droplets. The optimal time component of the standard waveform has been determined above, the optimal starting time of the damping waveform is approximately equal to the basic period of the velocity wave. At the same time, since the damping waveform t_{riseQ} and t_{fallQ} have a little influence on the residual oscillation, in order to simplify the waveform, t_{riseQ} and t_{fallQ} is set to be equal to t_{rise} and t_{fall} respectively. In this section, U_Q and t_{dwellQ} of the damping waveform are optimized.

(1) Voltage amplitude of the damping waveform U_Q

Set the voltage dwell time of the damping waveform t_{dwell} is 8μs, and U_Q varied from 1.8 V to 3 V, the step is 0.1V. Then obtain the nozzle inlet velocity curves corresponding to different damping waveform voltages. It can be seen from Figure 17 that with the gradual increase of the voltage U_Q, the residual oscillation of the pressure wave gradually attenuates. When U_Q is 2V, the residual oscillation of the pressure wave has the best damping effect. Therefore, U_Q=2V is chosen as the voltage amplitude of damping waveform.

(2) Dwelling time of the damping waveform voltage t_{dwellQ}

The dwelling time of the damping waveform voltage t_{dwellQ} was set to vary from 2μs to 12μs, the step was 2μs, and other parameters remained unchanged. The velocity curve of the nozzle inlet corresponding to voltage dwelling time was obtained. It can be seen from the Figure 18, with the gradual increase of

t_{dwellQ}, the damping effect on residual pressure wave increases at first and then decreases. When t_{dwellQ} is 8μs, the damping effect on residual pressure wave is the best, so the t_{dwellQ} is determined to be 8μs.

4.2 The effects of residual oscillation suppression

The optimized vibration damping waveform was loaded on the piezoelectric print head, and then obtained the speed-time curve of the nozzle inlet, as is shown in Figure 19. With the standard waveform, the time when the residual peak of nozzle inlet velocity is less than ± 5% of the maximum peak is 106 μs (red-dotted line position, the corresponding frequency is 9.43 kHz). While with the damping waveform, the time when the residual peak of nozzle inlet velocity is less than ± 5% of the maximum peak is 55 μs (red-solid line position, the corresponding frequency was 18.2 kHz). In the piezoelectric print head model, the operating frequency with damping waveform is about one time higher than that of the standard waveform.

As shown in Figure 20, eight ink droplets are continuously ejected at the operating frequency of 18 kHz, and compared the entrance velocity in the nozzle with the standard waveform and the damping waveform. When ink droplets are ejected with the standard drive waveform, the remaining pressure wave will not stop immediately, but will decay in oscillation. Therefore, the initial condition of the next driving waveform is different from the previous one. The pressure waves are superimposed and offset each other, resulting in the change of the peak velocity of the nozzle inlet, which leads to the different velocity of the ink drops, and ultimately leads to the decline of the printing accuracy. However, when the ink drops are injected with the damping waveform, the difference between the peak velocity of the nozzle inlet is almost negligible, which indicates that the vibration suppression waveform can effectively suppress the residual oscillation of the pressure wave, and ensure each droplet has similar initial conditions before injection, and effectively improve the printing accuracy and efficiency.

In the printing process, the droplets should be injected at different frequencies as required, and the droplets velocity should be constant. For this, the function of droplets velocity relative to injection frequency (DOD frequency) is introduced. Two droplets are ejected continuously at different frequencies, and the maximum fluid velocity of the second droplet was obtained which with the standard waveform and the damping waveform, as is shown in Figure 21. It can be seen that, driven by the standard waveform, with the increase of DOD frequency, the fluctuation of the maximum velocity of the fluid at the nozzle orifice is greater. That is, the velocity and volume of the droplets generated will change greatly with different injection frequencies. Applied with the damping waveform, it can be found that the maximum velocity of the fluid changed a little with the increase of DOD frequency, and the maximum velocity remains stable. This also means that the velocity and volume of the ink droplets finally formed have good consistency with different injection frequencies, indicating that the damping waveform has a good effect on suppressing residual oscillations.

In order to show the effect of damping waveform on improving working frequency and droplet consistency directly, the simulation analysis of the droplet ejection with the standard waveform and the damping waveform is performed. As shown in Figure 22 (a), when the standard waveform was loaded,

the residual oscillation of the pressure wave in the first period caused serious interference to the injection of droplets in the second period, resulting in a significant difference in the volume of droplets injected in the two periods (first droplet:22pl/second droplet 10.4pl). As shown in figure 22 (b), when the damping waveform was loaded, the two droplets are in good consistency in two periods (first period 22PL / second period 21.7PL). The results show that the damping waveform can effectively suppress the residual vibration of the pressure wave and greatly improve the working frequency and printing accuracy of the inkjet printing head.

5 Conclusions

(1) The piezoelectric inkjet print head model was developed, and the effects of trapezoidal driving waveform on the jetting characteristic were studied. Then nozzle entrance velocity and pressure corresponding to different voltage rise time t_{rise}, voltage falling time t_{fall} and voltage dwell time t_{dwell} are obtained, and each time component of the driving waveform was optimized. Finally, the time components of the driving waveform t_{rise}, t_{dwell} and t_{fall} were chosen as 4μs,8μs,3μs individually.

(2) The two-phase flow model was built and used to analyze the influence of driving parameters such as driving voltage amplitude, voltage dwell time, and operating frequency on the droplet ejection characteristics. Then the droplet speed and volume characteristics with different driving parameters were obtained.

(3) The effects of residual oscillation of pressure waves were studied, and the vibration suppression waveform was designed based on the principle of superposition of waves. The voltage amplitude and voltage dwell time of the suppression waveform was ascertained. Ultimately, the time components of the damping waveform were achieved. That is, T_{riseR}=4 μs, T_{dwellR}=8 μs, T_{fallR}=3 μs, T_{dwell}=16 μs, T_{riseQ}=4 μs, T_{dwellQ}=8 μs, T_{fallQ}=3 μs, U_R=20 V, U_Q =2 V. It is showed that the damping waveform can effectively suppress the residual oscillation, and improve the efficiency and stability of droplet injection obviously.

Abbreviations

T_{rise} Voltage rise time

T_{dwell} Voltage dwell time

T_{fall} Voltage falling time

T_{rR} Voltage rise time of the standard waveform

T_{fR} Voltage falling time of the standard waveform

T_{dR} Voltage dwell time of the first standard waveform

T_d The time interval between the damping waveform and the standard waveform

T_{dQ} Voltage dwell time of the damping waveform

T_{rQ} Voltage rise time of the damping waveform

T_{fQ} Voltage falling time of the damping waveform

U_R Voltage amplitudes of the standard waveform

U_Q Voltage amplitudes of the damping waveform

DOD Direction-of-departure

Declarations

AVAILABILITY OF DATA AND MATERIAL

Please contact author for data requests.

ACKNOWLEDGEMENTS

Not applicable.

FUNDING

This research was funded by the key scientific research project of Shaanxi Provincial Department of Education, "Research on Dynamic Stability and Intelligent Operation and Maintenance Technology of High-speed Printing and Packaging Equipment" (No.:20JY054)

AUTHOR INFORMATION

Affiliations

Faculty of Printing, Packing and Digital Media Technology, Xi' an University of Technology, Xi' an, 710048

WU Qiu-min, CUI Xin-yu, XU Lei, SU Xin

Contributions

All authors were involved in the writing of the manuscript and in the interpretation of the results. WQM and CXY performed the modelling and simulation of driving waveform and the structure of print head. XL assisted with the simulation of driving waveform, and SX revised the manuscript and made some improvements. All authors read and approved the final manuscript.

Corresponding author

Correspondence to CUI Xin-yu.

COMPETING INTERESTS

The authors declare no competing financial interests.

References

[1] S. Madhusudan, H.M. Haverinen, D. Parul, G.E. Jabbour, Inkjet printing-process and its applications, Adv. Mater. 22 (6) (2010) 673–685.

[2] H. Sirringhaus, T. Kawase, R.H. Friend, T. Shimoda, M. Inbasekaran, W. Wu, E.P. Woo, High-resolution inkjet printing of all-polymer transistor circuits, Science 290 (5499) (2000) 2123–2126.

[3] M. Nakamura, A.F. Kobayashi, A. Watanabe, Y. Hiruma, K. Ohuchi, Y. Iwasaki, M. Horie, I. Morita, S. Takatani, Biocompatible inkjet printing technique for designed seeding of individual living cells, Tissue Eng. 11 (11–12) (2005) 1658.

[4] B. Derby, N. Reis, Inkjet printing of highly loaded particulate suspensions, MRS Bull. 28 (11) (2003) 815–818. 7

[5] K. Li, J.K. Liu, W.S. Chen, L. Zhang, Controllable printing droplets on demand by piezoelectric inkjet: applications and methods, Microsyst. Technol. 24 (2) (2018) 879–889.

[6] R.E. Saunders, B. Derby, Inkjet printing biomaterials for tissue engineering: bioprinting, Int. Mater. Rev. 59 (2014) 430–448.

[7] R.D. Boehm, P.R. Miller, S.L. Hayes, N.A. Monteiro-Riviere, R.J. Narayan, Modification of microneedles using inkjet printing, AIP Adv. 1 (2) (2011) 22139.

[8] Chen Y S, Huang Y L, Kuo C H, et al. Investigation of design parameters for droplet generators driven by piezoelectric actuators[J]. International Journal of Mechanical Sciences, 2007, 49(6): 733-740.

[9] Gan H Y, Shan X, Eriksson T, et al. Reduction of Droplet Volume by Controlling Actuating Waveforms in Ink-jet Printing for Micro-pattern Formation[J]. Journal of Micromechanics & Microengineering, 2009, 19(5): 1-8.

[10] Shin P H, Sung J Y, Lee M H. Control of droplet formation for low viscosity fluid by double waveforms applied to a piezoelectric inkjet nozzle[J]. Microelectronics Reliability, 2011, 51(4): 797-804.

[11] Khalate A A, Bombois X, Babuška R, et al. Performance improvement of a drop-on-demand inkjet printhead using an optimization-based feedforward control method[J]. Control Engineering Practice, 2011, 19(8): 771-781.

[12] XU Lei. Research on piezoelectric inkjet jet characteristics and residual oscillation suppression[D]. Xi' an University of Technology,2021.

Figures

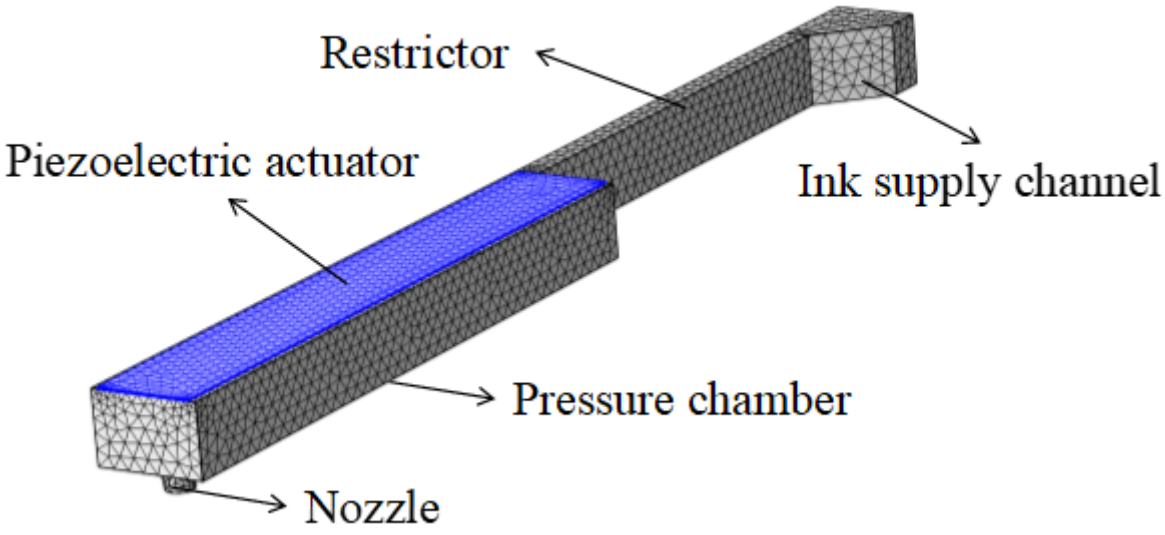

Figure 1

Finite element analysis model of the piezoelectric inkjet print head

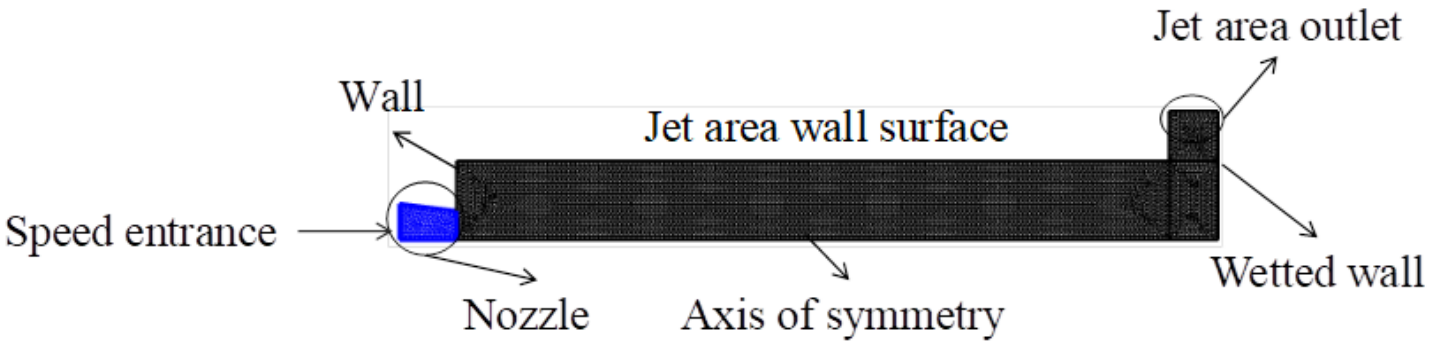

Figure 2

Two-phase flow finite element analysis model

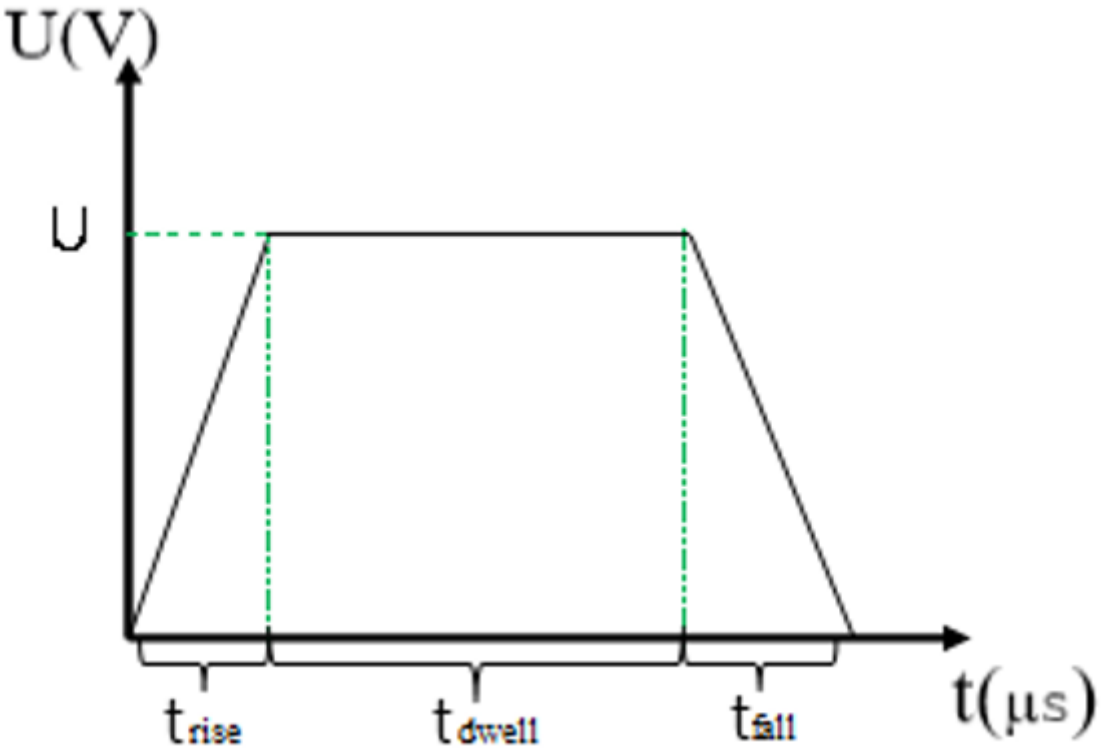

Figure 3

Positive polarity single trapezoidal drive waveform

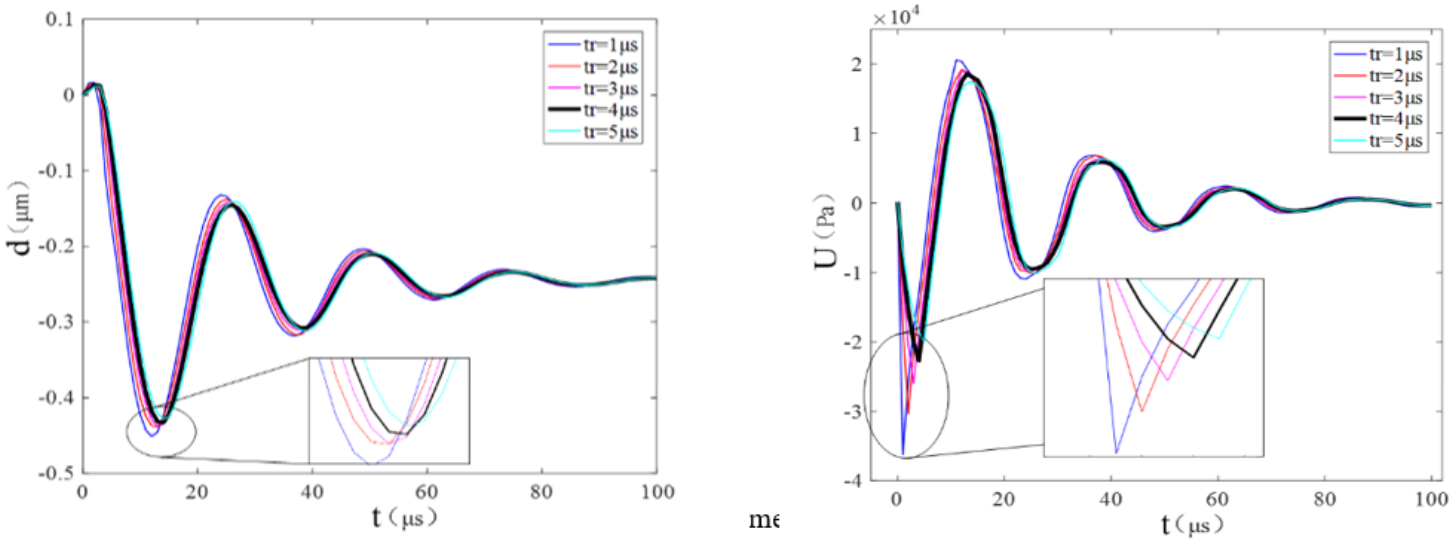

Figure 4

The pressure-time curve at the nozzle orifice corresponding to different t_{rise} values

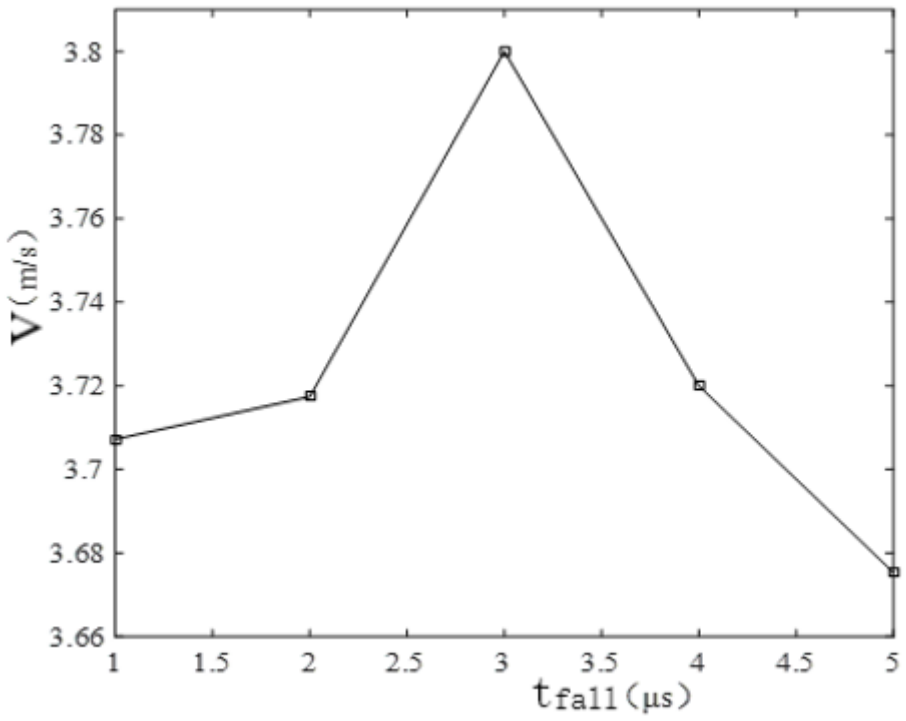

Figure 5

The peak value of the average fluid velocity at the nozzle orifice

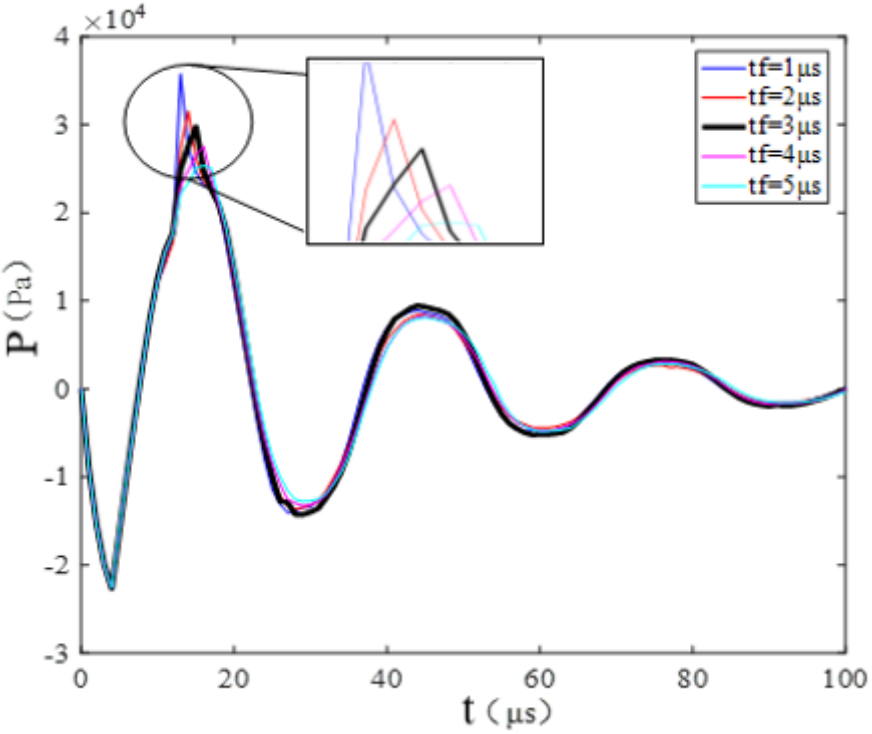

Figure 6

The pressure change curve at the inlet of the nozzle orifice corresponding to different t_{fall} values

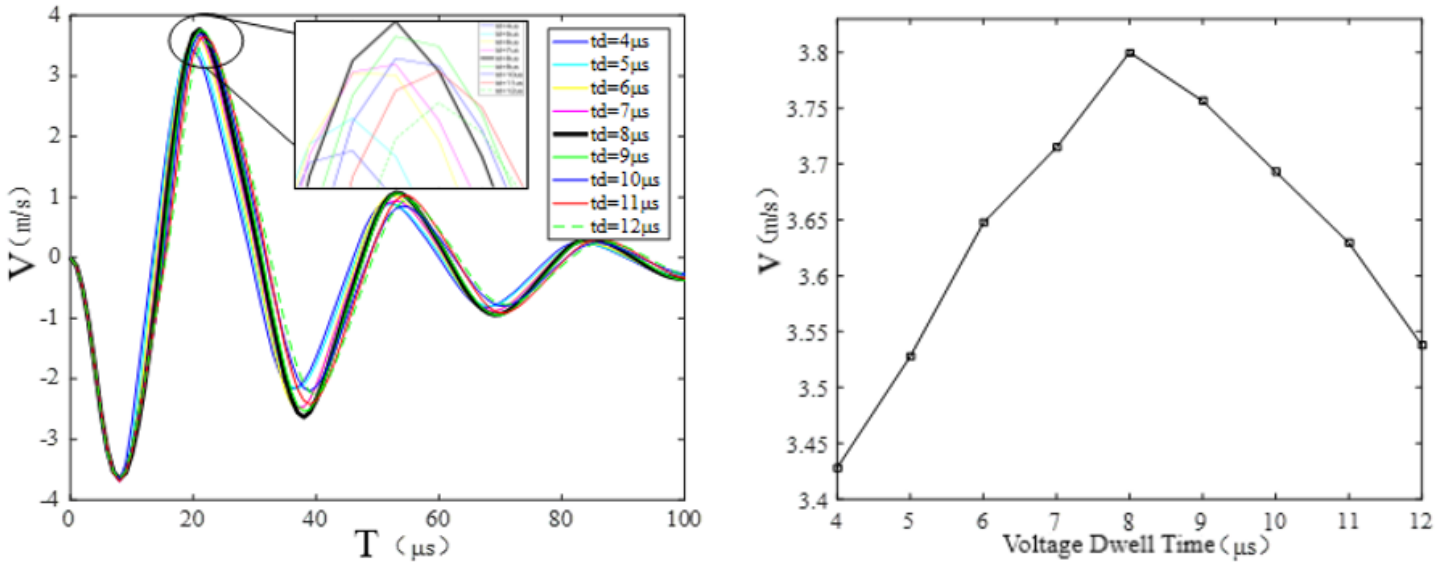

Figure 7

The velocity-time curve at the nozzle orifice corresponding to the t_{dwell} of different voltages and the corresponding peak fluid velocity curve at the nozzle orifice

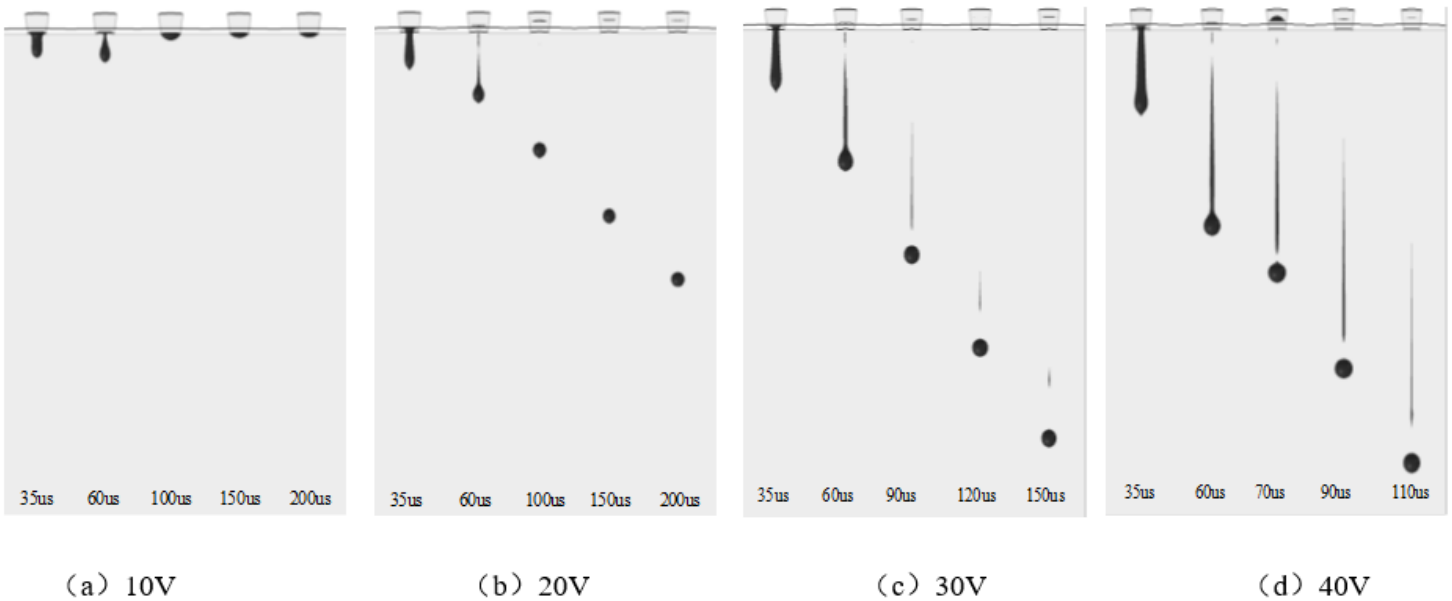

Figure 8

The influence of driving voltage amplitude on injection effect

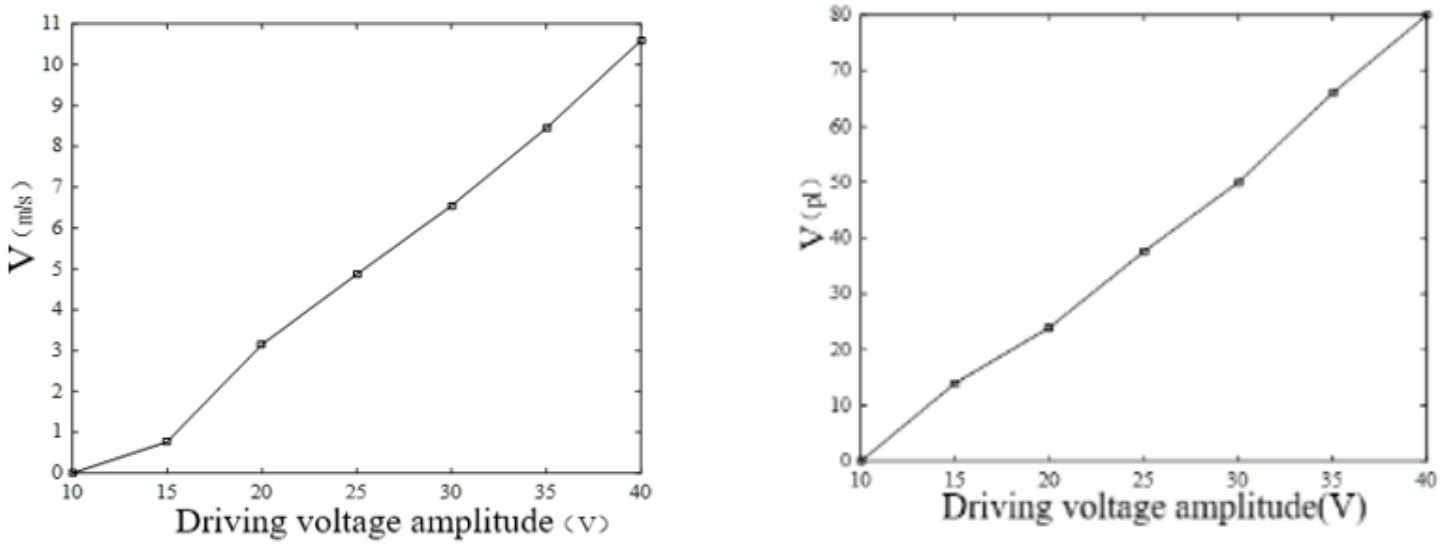

Figure 9

The relationship between driving voltage and ink droplet flying speed and volume

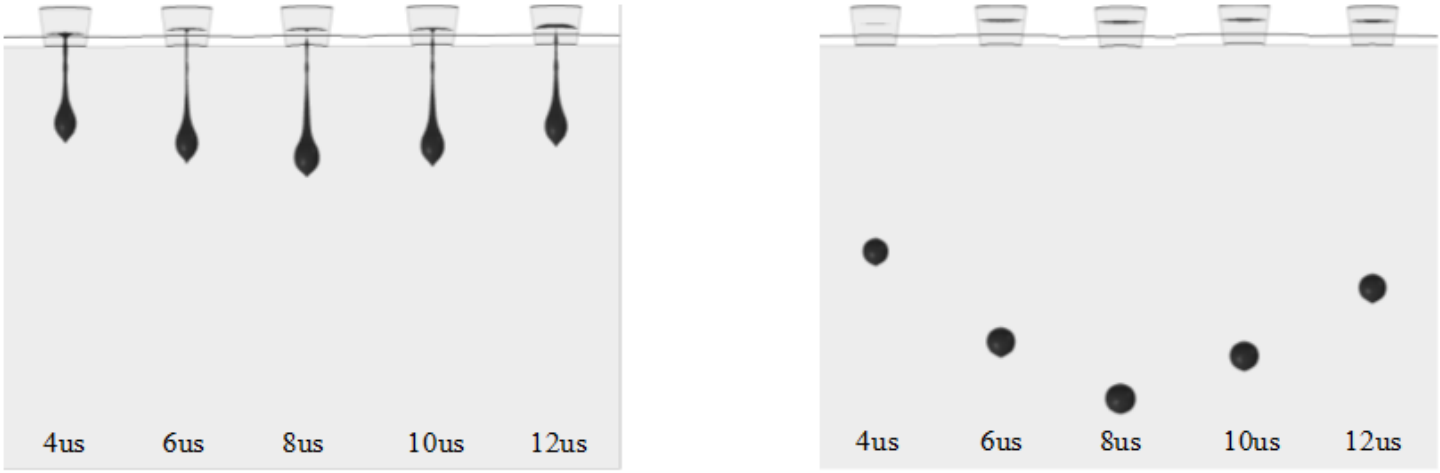

(a) 40μs (b) 150μs

Figure 10

Comparison of ink drop formation with different voltage dwell time

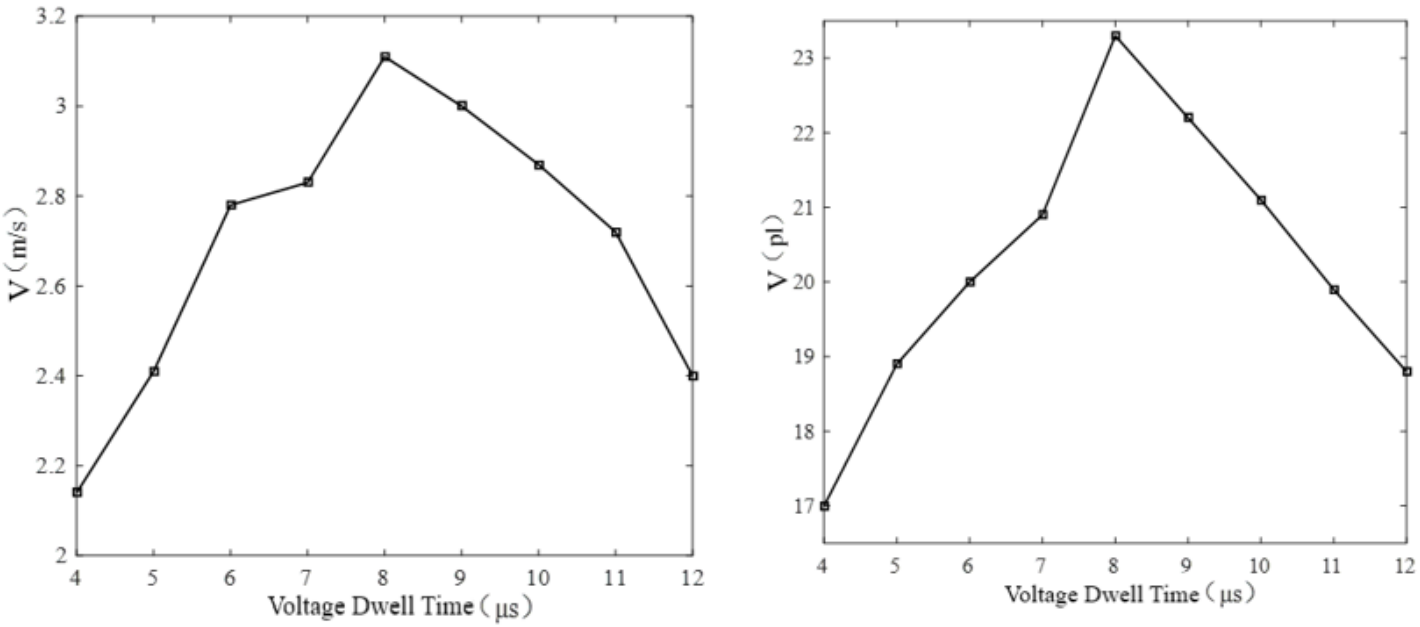

Figure 11

The relationship between the voltage dwell time and the flying speed and volume of droplets

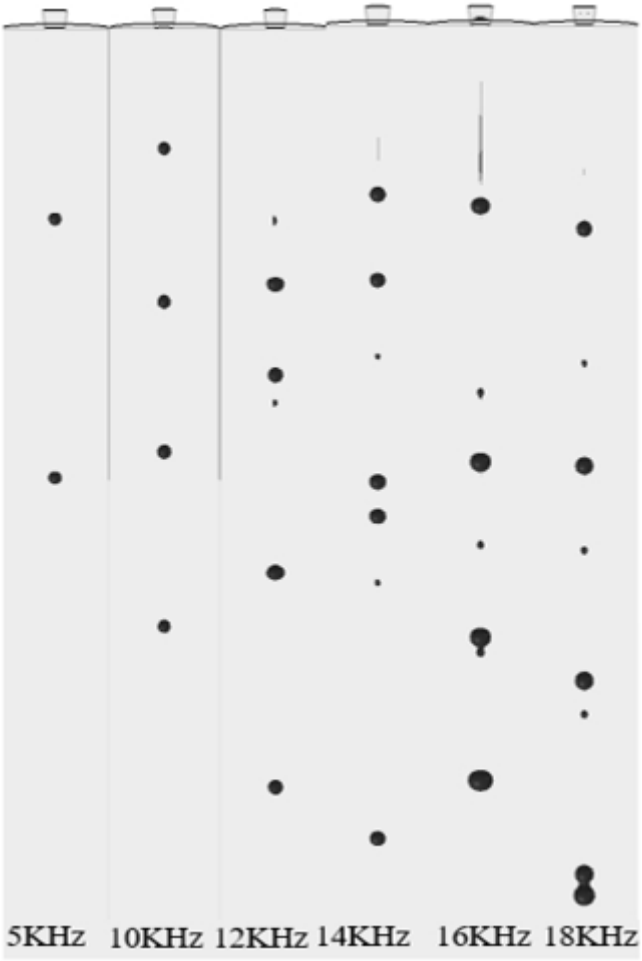

Figure 12

The jetting effect of droplets with different operating frequencies

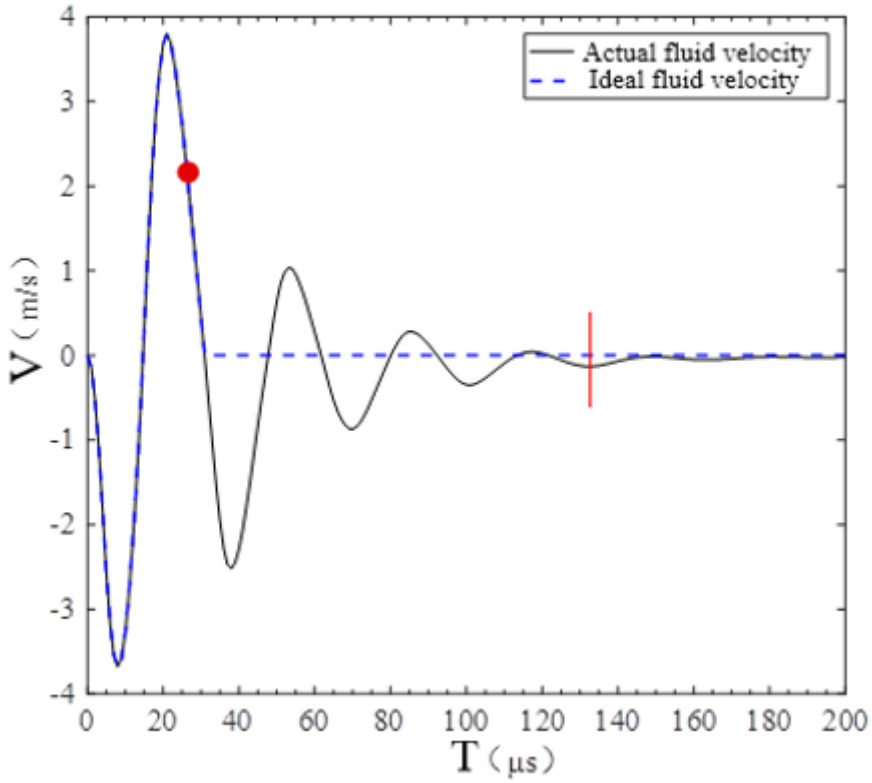

Figure 13

Comparison of the fluid velocity at the nozzle orifice

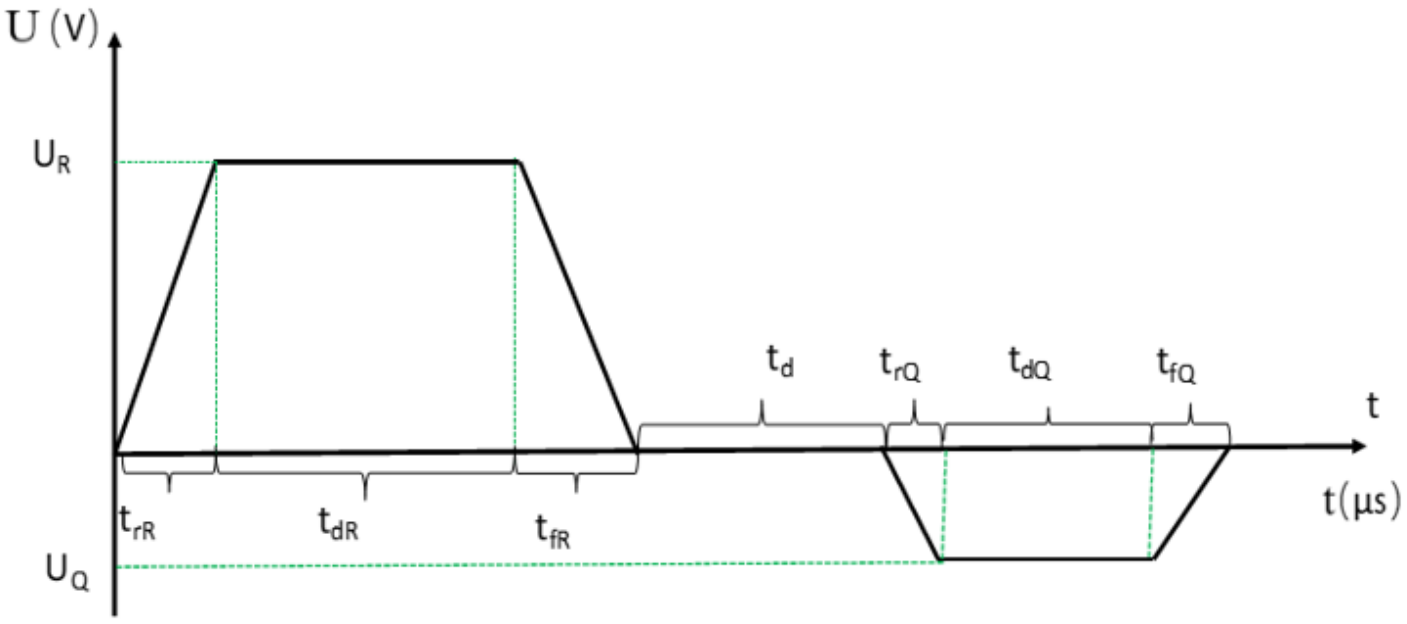

Figure 14

Anti-vibration waveform

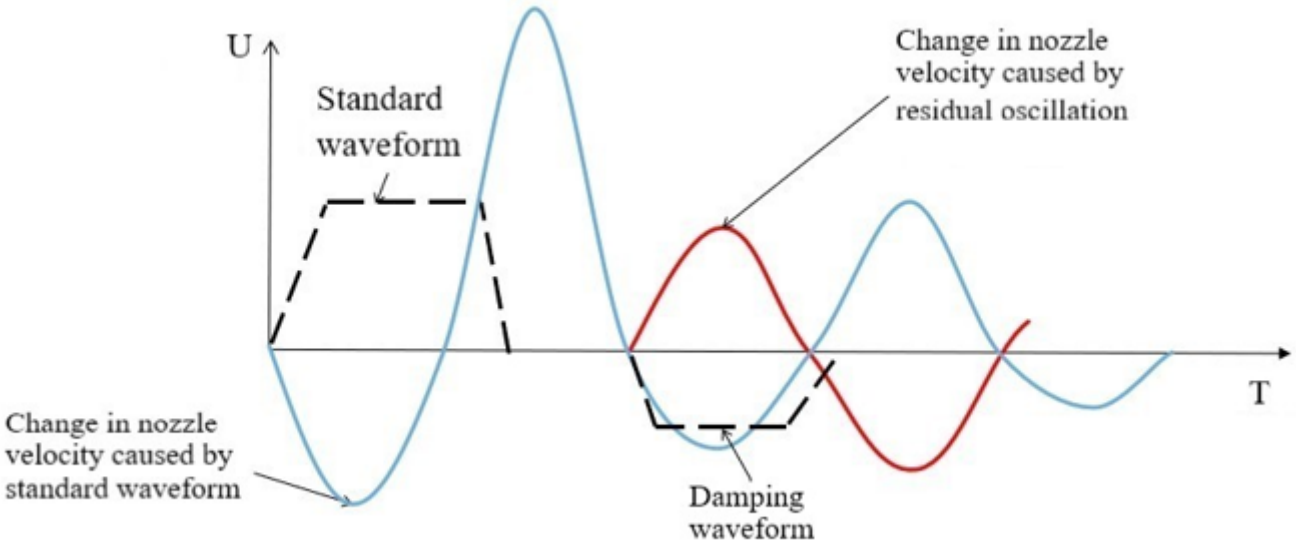

Figure 15

Schematic diagram of velocity wave superposition and cancellation

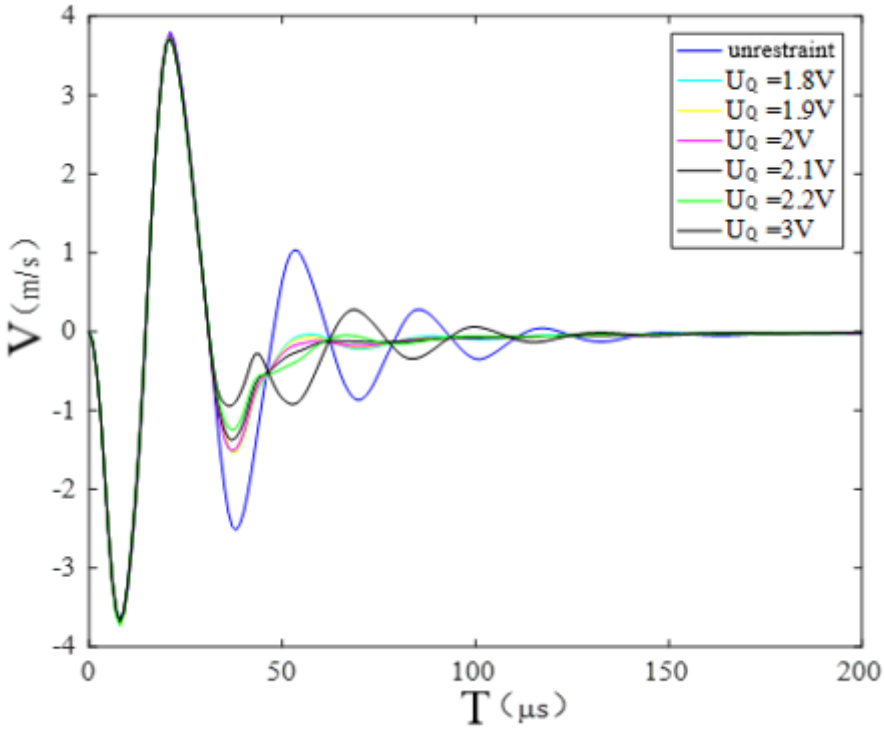

Figure 16

The fluid velocity-time curve at the nozzle orifice corresponding to different suppression waveform voltages

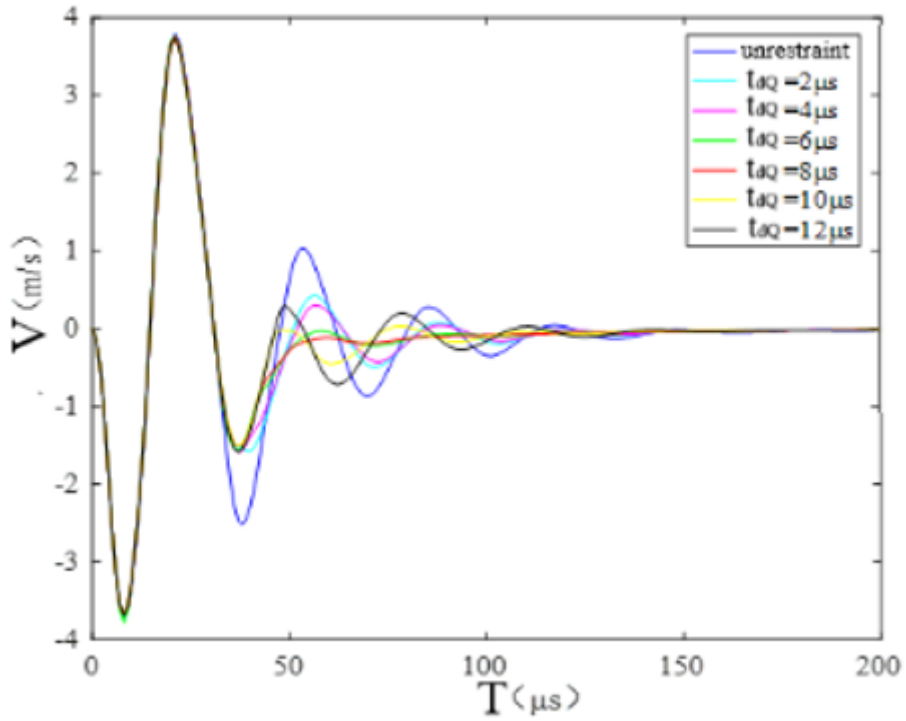

Figure 17

The fluid velocity-time curve at the nozzle orifice corresponding to the t_{dwell} of different suppression waveform voltages

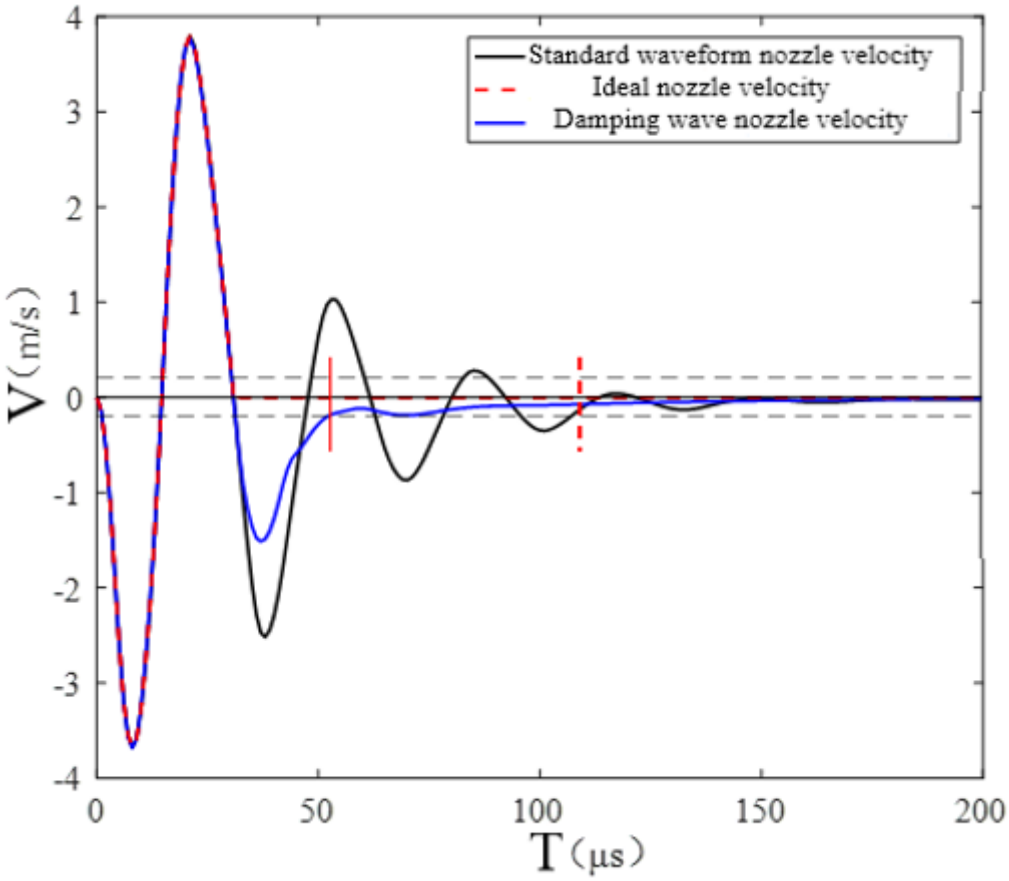

Figure 18

Fluid velocity-time curve at the nozzle before and after applying suppression waveform

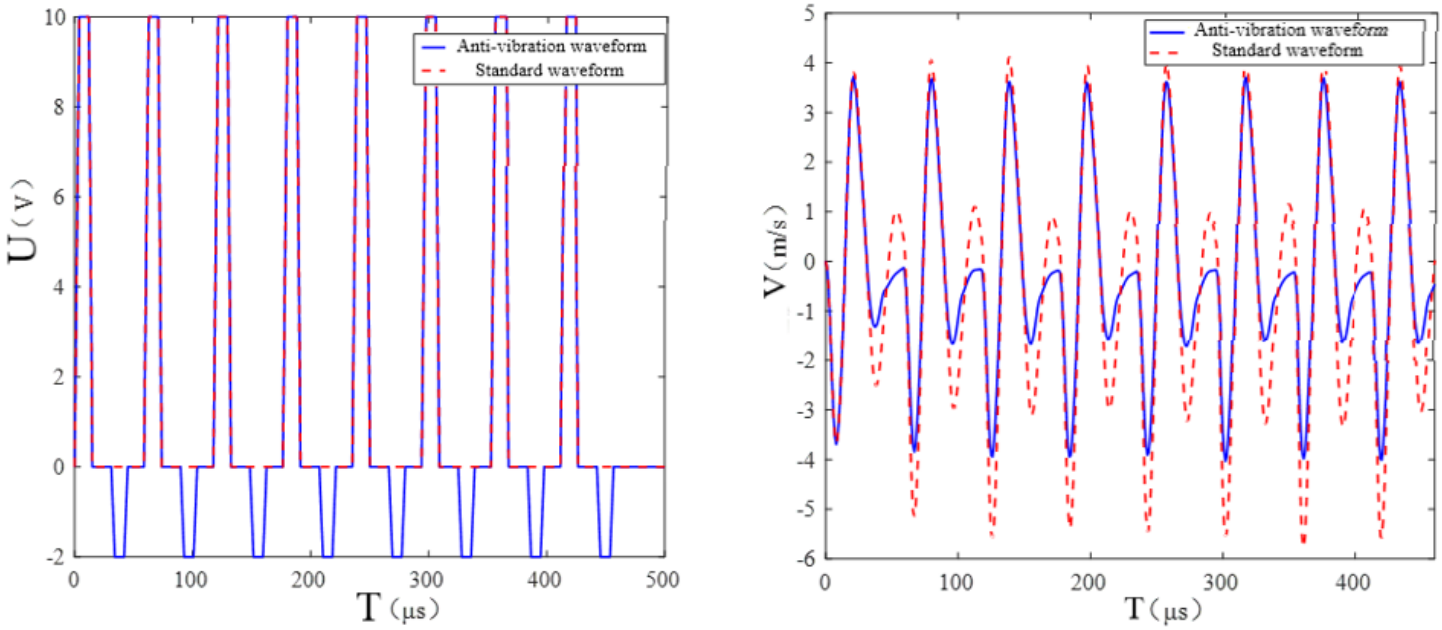

Figure 19

The driving waveform and the corresponding fluid velocity-time curve at the nozzle orifice when eight ink droplets are continuously ejected at a frequency of 20 kHz

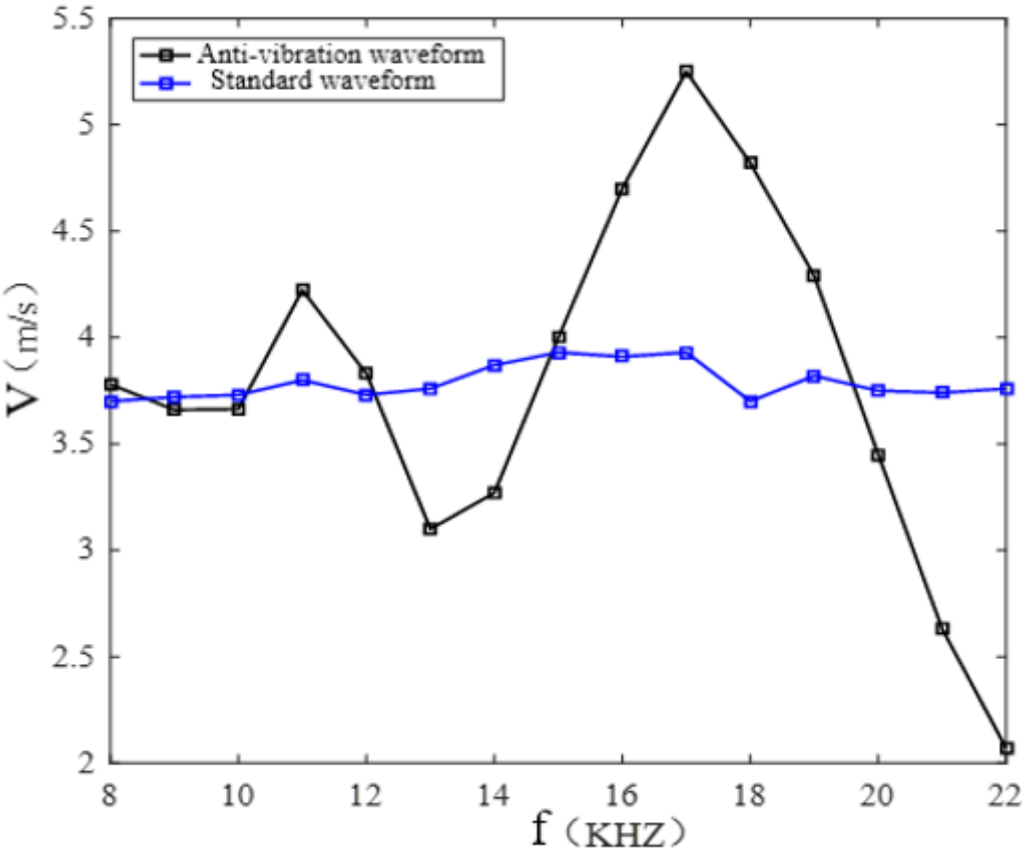

Figure 20

The peak fluid velocity at the nozzle orifice at different injection frequencies

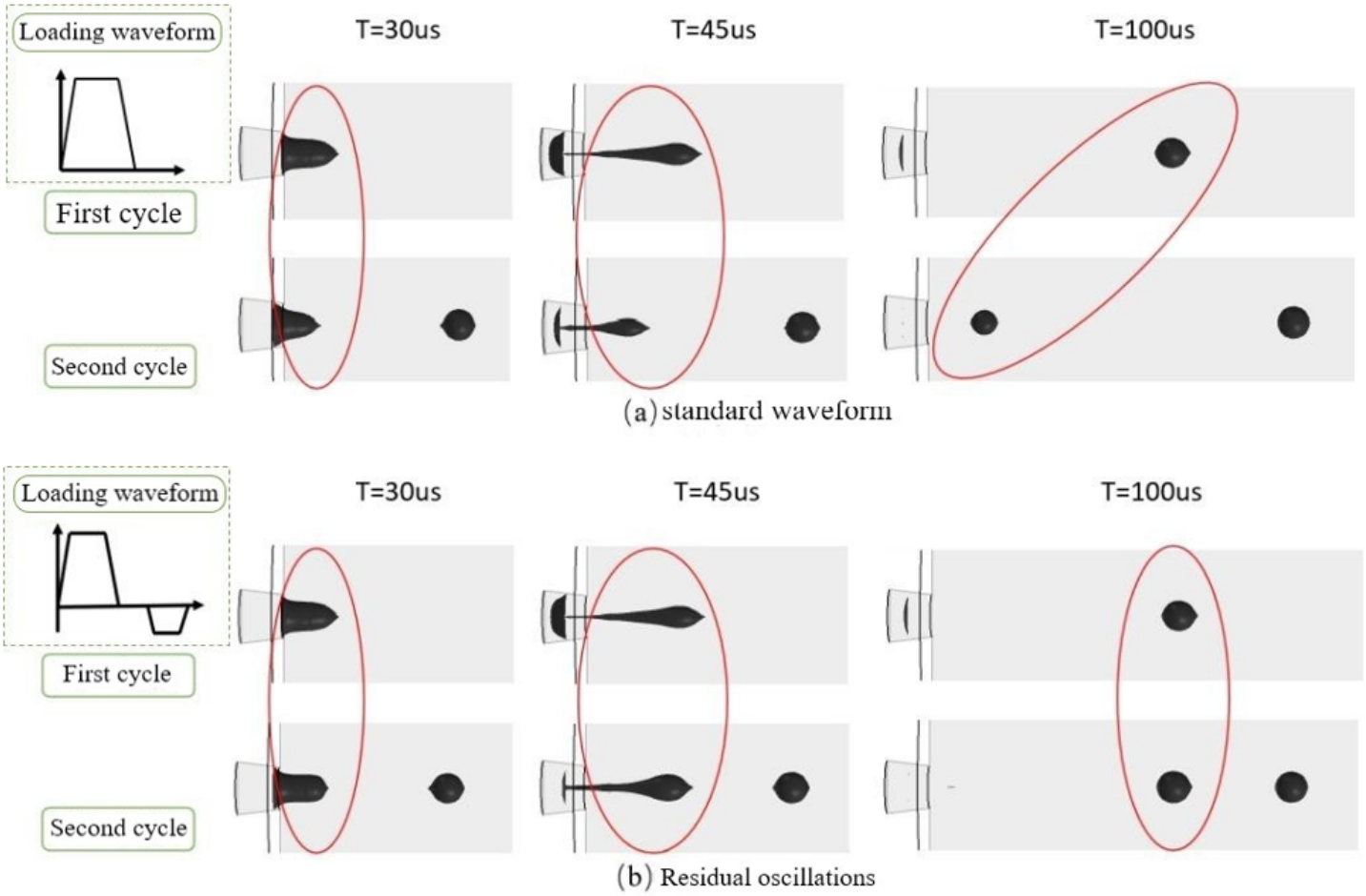

Figure 21

The ejection status of ink droplets in two cycles of the piezoelectric inkjet print head when different driving waveforms are loaded